Discovery of a Conditionally Activated IL-2 that Promotes Antitumor Immunity and Induces Tumor Regression

Christopher J. Nirschl, Heather R. Brodkin, Daniel J. Hicklin, Nesreen Ismail, Kristin Morris, Cynthia Seidel-Dugan, Philipp Steiner, Zoe Steuert, Jenna M. Sullivan, Ethika Tyagi, William M. Winston, and Andres Salmeron

ABSTRACT

IL-2 is a cytokine clinically approved for the treatment of melanoma and renal cell carcinoma. Unfortunately, its clinical utility is hindered by serious side effects driven by the systemic activity of the cytokine. Here, we describe the design and characterization of a conditionally activated IL-2 prodrug, WTX-124, that takes advantage of the dysregulated protease milieu of tumors. WTX-124 was engineered as a single molecule containing an inactivation domain and a half-life extension domain that are tethered to a fully active IL-2 by protease-cleavable linkers. We show that the inactivation domain prevented IL-2 from binding to its receptors in nontumor tissues, thereby minimizing the toxicity associated with systemic exposure to IL-2. The half-life extension element improves the pharmacokinetic profile of WTX-124 over free IL-2, allowing for greater exposure. WTX-124 was preferentially activated in tumor tissue by tumor-associated proteases, releasing active IL-2 in the tumor microenvironment. *In vitro* assays confirmed that the activity of WTX-124 was dependent on proteolytic activation, and *in vivo* WTX-124 treatment resulted in complete rejection of established tumors in a cleavage-dependent manner. Mechanistically, WTX-124 treatment triggered the activation of T cells and natural killer (NK) cells, and markedly shifted the immune activation profile of the tumor microenvironment, resulting in significant inhibition of tumor growth in syngeneic tumor models. Collectively, these data demonstrate that WTX-124 minimizes the toxicity of IL-2 treatment in the periphery while retaining the full pharmacology of IL-2 in the tumor microenvironment, supporting its further development as a cancer immunotherapy treatment.

See related Spotlight by Silva, p. 544.

Introduction

Cancer immunotherapy has rapidly established itself as the fourth pillar of cancer treatment largely owing to the clinical success of checkpoint inhibitors (1–3). Despite the durable responses achieved by some patients using these new therapies, the proportion of responders is still relatively low and restricted to only some cancer types. Tumor mutational burden, the presence or absence of T-cell infiltration, and the overall immunosuppressive microenvironment of tumors greatly influences the response to immunotherapies. Although immune checkpoint blockade can prevent the physiologic stop signal that arises in response to immune activation, other approaches can be used to positively stimulate the antitumor immune response. One approach involves the use of immune-activating cytokines. Numerous preclinical and clinical studies have demonstrated the promise of cytokine therapy to increase antitumor immunity. In fact, these were some of the first cancer immunotherapies approved for clinical use. However, systemic toxicity and poor pharmacokinetic profiles have limited their clinical application (4).

IL-2 is a critical cytokine driving the immune-mediated killing of cancer cells. Its mechanism of action includes stimulation of both innate and adaptive immune cells. The IL-2 receptor (IL-2R) is composed of three subunits: CD25 (IL-2Rα), CD122 (IL-2Rβ), and CD132 (IL-2Rγ). Signal transduction is mediated through a heterodimer of CD122 and CD132. Together, these molecules form the IL-2 medium-affinity receptor, which is expressed on natural killer (NK) cells, monocytes, macrophages, and resting $CD4^+$ and $CD8^+$ T cells. The trimeric IL-2 high-affinity receptor (CD25/CD122/CD132) is present on activated T and NK cells and constitutively expressed on $CD4^+FoxP3^+$ regulatory T cells (Treg). IL-2 increases the proliferation and activation of T cells and NK cells and induces the differentiation of $CD8^+$ T cells into effector and memory cells (5, 6). Recombinant human IL-2 (proleukin) is approved for clinical use in metastatic melanoma and renal cell carcinoma as a high-dose therapy, but this treatment is associated with serious side effects, including vascular leakage syndrome (VLS) and hypotension, limiting its practical use (5, 7).

To address the limitations of IL-2 high-dose therapy, several approaches have been pursued to develop next-generation IL-2 molecules that only bind the medium-affinity receptor (CD122/CD132) in the hope of alleviating toxicities and reducing the activation of Tregs (7–10). However, many of these molecules still activate IL-2 receptors on nontumor specific immune cells located in healthy tissues and therefore, may not minimize toxicities associated with systemic IL-2 administration. Molecules that block IL-2 signaling in the periphery while delivering a fully active native IL-2 in the tumor microenvironment (TME) may be a more

Werewolf Therapeutics, Cambridge, Massachusetts.

Note: Supplementary data for this article are available at Cancer Immunology Research Online (http://cancerimmunolres.aacrjournals.org/).

Corresponding Authors: Cynthia Seidel-Dugan, Werewolf Therapeutics, 1030 Massachusetts Ave, Cambridge, MA 02138. Phone: 617-952-0542; Fax: 617-354-0510; E-mail: cseideldugan@werewolftx.com; and Andres Salmeron, asalmeron@werewolftx.com

Cancer Immunol Res 2022;10:581–96

doi: 10.1158/2326-6066.CIR-21-0831

appropriate approach to achieve the full potential of IL-2 antitumor activity with minimal systemic toxicities.

WTX-124 is composed of a conditionally activated IL-2 molecule, referred to as an IL-2 INDUKINE protein, which utilizes the dysfunctional protease microenvironment in the tumor (11, 12). This molecule was designed to be an inactive cytokine prodrug that is conditionally activated in the TME to release IL-2. The WTX-124 protein was engineered as a single molecule that contains IL-2, an inactivation domain, and a half-life extension domain. We found that the inactivation domain blocked the binding of WTX-124 to IL-2 receptors in circulation and normal tissues. The half-life extension domain supported infrequent systemic administration and enabled biologically relevant exposures in tumor tissue. The inactivation and half-life extension domains are linked to IL-2 via a tumor protease-sensitive linker. The linker sequence for WTX-124 was selected by a screen utilizing a diverse set of primary human tumor samples to deliver a sequence that was processed by the majority of the tumor types screened but was not proteolytically cleaved by normal primary human cells. We found that once WTX-124 reached the tumor, tumor-associated proteases cleaved the linkers and released the fully active IL-2 selectively in the TME.

WTX-124 contains a native, wild-type IL-2 that retains binding to the high-affinity IL-2 receptor. Therefore, delivery of fully potent IL-2 locally to the TME is expected to fully activate and amplify target effector T-cell populations. This might be an important antitumor strategy, as suggested by an analysis of the clonal content and activation state of $CD8^+$ T cells in patients with basal cell carcinoma. After a positive response to anti-programmed cell death 1 (PD-1) therapy, the basal cell carcinoma tumors went through clonal replacement, where most of the activated/exhausted T cells found after treatment were newly identified clones that were absent prior to treatment (13). These new key effector cells will transiently express the IL-2 high-affinity receptor (CD25/CD122/CD132) during expansion and will benefit from the presence of fully active IL-2 to overcome a naturally suppressive TME. The selective release of IL-2 in the tumor by WTX-124 has the potential to transform the suppressive microenvironment and tip the balance toward an antitumor immune response while avoiding systemic toxicities.

Materials and Methods

Cell lines

All cell lines were grown and maintained by Charles River Laboratories according to ATCC guidelines and kept in culture for no longer than 2 weeks. The MC38 cell line was obtained from the NCI Fredrick Cancer DCT Tumor Repository in 2012 and the B16-F10 cell line was purchased from ATCC in May of 2019. Both cell lines were tested for *Mycoplasma* every 2 months and have not been reauthenticated within the past year. Frozen MC38 or B16-F10 cells were thawed and maintained for 1–3 passages before implantation. B16-F10 was cultured in RPMI-1640 with L-Glutamine (Gibco, 11875-085) with 10% heat-inactivated FCS (Gibco, 35-015-CV) whereas MC38 was cultured in DMEM (Gibco, 1966-025) supplemented with 10% heat-inactivated FCS (Gibco, 16000-044). Prior to tumor implantation, cells were washed twice with PBS and counted.

Mice, tumor implantations, and *in vivo* dosing

All mouse *in vivo* work was performed in accordance with current regulations and standards of the U.S. Department of Agriculture and the NIH at Charles River Laboratories with the approval of an Institutional Animal Care and Use Committee. Female, 6 to 8 weeks old C57Bl/6 mice from Charles River Laboratories were shaved on their flank 1 day prior to tumor cell implantation. A total of 5×10^5 MC38 or 1×10^5 B16-F10 cells were injected subcutaneously and monitored for tumor growth. Extra mice were implanted to have sufficiently sized tumors for randomization. Tumor volume was monitored until the group average was 100 to 150 mm^3, and mice were randomized into treatment groups on day 0. Mice receiving any INDUKINE proteins were dosed twice a week. INDUKINE proteins used in these studies included WTX-124, WW0177, and WW0057. WW0177 is a variant of WTX-124 that does not include the inactivation domain, whereas WW0057 is a variant of WTX-124 that does not contain the half-life extension domain. Mice receiving recombinant human IL-2 (rhIL-2 or WW0196) were dosed twice a day for 5 days before receiving a 2-day break (5/2 regimen) and the cycle was repeated. rhIL-2 was produced in house (WW0196). The doses of the INDUKINE proteins or rhIL-2 (WW0196) used in these studies are specified in the article and in the individual figure legends. In studies where PD-1 blockade was used, mice were dosed with anti-PD-1 (200 μg/dose, clone RMP1-14, BioXCell) on a twice-weekly schedule. In studies using FTY720 (Sigma-Aldrich, SML0700-25MG), mice were initially dosed with 25 μg on the first dose, then treated daily with 10 μg per dose throughout the course of the experiment. All treatments were administered by intraperitoneal injection, and mice were dosed for 2 weeks unless otherwise noted. Body weight and tumor volume were both measured twice weekly for the duration of the study. Tumors were measured in two dimensions using calipers, and volume was calculated using the formula: $Tumor\ volume\ (mm^3) = [(w^2 \times l)/2]$ where $w =$ width and $l =$ length, in mm, of a tumor. Mice were kept on study until tumors reached 1,500 mm^3, or the study reached the termination point at day 45. In some instances, mice with complete regressions were saved for later memory experiments.

Murine VLS model

Murine VLS experiments were performed in accordance with current regulations and standards of the U.S. Department of Agriculture and the NIH at Biomodels LLC. Female, 8 to 10 weeks old C57Bl/6 mice were dosed with equimolar amounts of either rhIL-2 (100 μg/dose, given seven times over 4 days), WW0177 (given twice on day 0 and day 3 at 30 μg per dose), or an IL-2 INDUKINE molecule (given twice on day 0 and day 3, at 59 μg per dose) by intraperitoneal injection. On day 3, animals were given intravenous injections of Evan's Blue dye (Sigma-Aldrich, E2129-10G), and animals were perfused 30 minutes later with 50 mL of saline with heparin at a rate of 10 mL/minute. Lungs were harvested and placed in formamide at 37°C for 24 hours. After 24 hours, Evan's Blue extravasation into the lungs was assessed by measuring the absorbance at 620 and 650 nm using a Spectra Max M2 Spectrophotometer (Molecular Devices) and comparing the absorbance values with a freshly prepared standard curve of Evan's Blue dye.

INDUKINE protein production, protease activation, and SDS-PAGE analysis

WTX-124, rhIL-2, WW0177, WW0057, and WTX-124-NC were produced at Werewolf Therapeutics. WTX-124 consists of native human IL-2 linked to a proprietary inactivation domain and a half-life extension domain by a proprietary linker sequence. The inactivation domain consists of a Fab antibody, whereas the half-life extension domain consists of a single-domain antibody targeting human (and murine) albumin, both of which were discovered by Werewolf Therapeutics. For additional details on INDUKINE designs, please refer to patent #10,696,724. The proteins were expressed using the Expi293

expression system from Life Technologies (A14635) according to the manufacturer's protocol. On day 4 posttransfection, the cultures were spun down, filtered with 0.2 μm bottle top filters, and left to rotate overnight in the presence of MabSelect resin (GE Healthcare, 17519902). The following day, the culture/resin mixture was applied to a gravity column and the resin was washed with PBS (TEKNOVA, endotoxin tested). Proteins were eluted with 200 mmol/L acetic acid pH 3.5, 50 mmol/L NaCl and neutralized with 1 mol/L Tris pH 8. Elutions were pooled, dialyzed, concentrated, aliquoted, and stored for future use at −80°C. WTX-124 was dialyzed into 20 mmol/L histidine pH 6, 150 mmol/L NaCl, whereas rhIL-2 and WW0177 were dialyzed against 1× PBS. Extinction coefficients were determined for each protein theoretically using SnapGene (v 5.0.7) and protein concentration was determined by A280. For SDS-PAGE gels, 3 μg of protein was loaded on a 16% Tris-Glycine gel (Thermo Fisher Scientific) under nonreducing conditions. In experiments where protease-activated INDUKINE proteins were used, INDUKINE protein was incubated with Cathepsin L (R&D Systems, 952-CY) at room temperature for 10 minutes, then frozen for later use. Intact INDUKINE protein was also incubated at room temperature without enzyme, then frozen as a control.

HEK-Blue IL-2 reporter assay

The HEK-Blue IL-2 reporter cell assay was performed according to the manufacturer's protocol (Invivogen, hkb-IL-2). On assay day 1, the cells were rinsed, resuspended in media containing 1.5% human serum albumin, and plated at a concentration of 5×10^4 cells per well in a 96-well flat bottom plate. Titrated amounts of intact and protease-activated (cleaved) INDUKINE proteins or rhIL-2 were added to the cells to generate a full dose–response curve. On day 2, secreted embryonic alkaline phosphatase levels were measured using a Synergy HTX multimode plate reader (Biotek) at 620 nmol/L according to the manufacturer's protocol.

Human and murine primary cell assays

Human peripheral blood mononuclear cells (PBMC) were isolated from whole blood (BioIVT) using Ficoll-Paque Plus (GE Healthcare, GE17-1440-03) according to the manufacturer's protocol and frozen in Recovery Cell Culture Freezing Media (Gibco, 12648010) for later use. To generate activated T cells (Tblasts), PBMCs were thawed, counted, and stimulated with 5 μg/mL of phytohemagglutinin (PHA; Sigma-Aldrich, L1668-5MG) for 72 hours before being frozen for later use. To measure intact or protease-activated (cleaved) INDUKINE protein activity, Tblasts were plated in a 96-well round bottom plate, and titrated amounts of intact or protease-activated (cleaved) INDUKINE proteins or rhIL-2 were added to the cells to generate a full dose–response curve. After 72 hours, proliferation was measured using Cell Titer glow reagent (Promega, G7570) according to the manufacturer's protocol. Luminescence was measured using a Perkin Elmer Enspire Alpha Reader with Enspire Manager Software (V4.13.3005.1482).

For murine Tblast experiments, previously frozen splenocytes from naïve C57Bl/6 mice (Jackson Labs) were thawed, washed, and stimulated with 2 μg/mL of Concanavalin A (Sigma-Aldrich, C2575) for 72 hours before being frozen in Recovery Cell Culture Freezing Media (Gibco). T-cell activation was performed in complete media [RPMI-1640 media (Gibco, 11875-093) supplemented with 10% heat-inactivated FBS (Gibco, 10082-142), 100 units/mL of penicillin (Gibco, 15140-122), 100 μg/mL streptomycin (Gibco, 15140-122) and 0.1% 2-mercaptoethanol (Gibco, 21985023)]. To measure INDUKINE protein activity, murine Tblasts were plated in a 96-well round bottom plate. Titrated amounts of intact or protease-activated (cleaved) INDUKINE protein or rhIL-2 were added to the cells to generate a full dose–response curve. After 72 hours, proliferation was measured using Cell Titer glow reagent (Promega) according to the manufacturer's protocol.

WTX-124 stability in murine plasma and human serum

Whole blood from 6 to 8 weeks old female C57Bl/6 mice was used to generate plasma. Human serum was purchased from BioIVT. On day 1 of the assay, WTX-124 was added to either the murine plasma or human serum before the samples were mixed and divided into three aliquots, which were incubated at 37°C for the indicated times before being frozen for later analysis. To assess the enzymatic processing of WTX-124, samples were thawed, and WTX-124 cleavage was assessed using Western blot analysis against human IL-2. Intact and protease-activated WTX-124 were included as positive and negative controls.

Western blot analysis was performed using the JESS system (Protein Simple) according to the manufacturer's protocol. The primary anti-human IL-2 was purchased from R&D Systems (AF-202-NA) and the anti-goat secondary was purchased from Jackson Labs (AB_2338513). Samples and antibodies were loaded into a 12–230 kDA Jess separation module and run using a Jess system set to the standard settings for chemiluminescence. Analysis of the resulting Western blot was performed using Compass for Simple Western Software (v4.1.0).

Pharmacokinetic analysis

In experiments where pharmacokinetic analysis was performed on MC38 tumor-bearing mice dosed with WTX-124, tumors were implanted and WTX-124 was dosed as described above, with dosing specified in the respective figure legend. Plasma and tumor samples were collected at indicated timepoints by Charles River Laboratories and shipped on dry ice to Werewolf Therapeutics where they were stored at –80°C. MC38 tumor lysates were generated by homogenizing each tumor with a Qiagen TissueRuptor homogenizer with disposable probes (Qiagen) in ice-cold Lysis Buffer [1X TBS (Sigma-Aldrich, T5912-1L), 1 mmol/L EDTA (Sigma-Aldrich, 3690-100 mL), 1% Triton X-100 (Sigma-Aldrich, X100-1000 mL)], with protease inhibitors (Sigma-Aldrich, P8340-1L) in diH_2O. Plasma and tumor lysates were analyzed using the BioLegend IL-2 ELISA (431804), which detects both intact WTX-124 as well as free IL-2, as per the manufacturer's instructions and analyzed using a Biotek Synergy Plate Reader running Gen 5 Software (Version 3.10). Intact WTX-124 was used to generate a 12-point standard curve. To specifically analyze the level of free IL-2, samples were measured using an IL-2 AlphaLISA (PerkinElmer, AL221C), which detects free human IL-2 but not intact WTX-124 due to competition with the inactivation domain. All AlphaLISAs were performed according to manufacturer's instructions and analyzed using a Perkin Elmer Enspire reader and Enspire Manager Software (V4.13.3005.1482).

Tumor digestions and NanoString analysis

MC38 and B16-F10 tumors were chopped into small pieces (<5 mm^3) in phenol-free RPMI-1640 (Thermo Fisher Scientific) before being enzymatically digested with Collagenase IV (3 mg/mL, Gibco, 17104019) at 37°C for 35 minutes while shaking. After digestion, tumor samples were mechanically dissociated through a 70 μm strainer. Single-cell suspensions were then counted and analyzed by flow cytometry. For NanoString analysis, 5×10^5 cells were frozen in 100 μL of RLT Lysis buffer (Qiagen, 1053393). RNA samples were shipped to LakePharma and analyzed using the nCounter Mouse PanCancer Immune Profiling Codeset Panel with the nCounter FLEX

analysis system. NanoString analysis was performed using nSolver Software with the Advanced Analysis module installed.

Flow cytometry

All cell staining was performed in 96-well round bottom plates using FACs Buffer (PBS + 0.5% BSA) or 1× Permeabilization Buffer (eBioscience, 00-5223-56) where appropriate. Cells were first treated with FC block (BioLegend, 101320) at room temperature before tetramer staining was performed for 20 minutes at room temperature. After tetramer staining, cells were washed and then stained with a master mix of extracellular antibodies for 20 minutes at 4°C. Cells were then washed and fixed/permeabilized overnight using the eBioscience Foxp3 Transcription Factor Staining Buffer Set according to the manufacturer's protocol. The next day, samples were washed with Perm Buffer and stained with intracellular markers for 20 minutes at 4°C. Cells were then washed and analyzed on a Cytek Aurora system. Fluorescence minus one and single-stain controls were included for all stains. In some instances, OneComp ebeads (Thermo Fisher Scientific, 01-1111-42) were stained alongside cells to act as single-stain controls. When flow cytometry was used to assess effector cytokine production, cells were restimulated with phorbol 12-myristate 13-acetate (PMA; 50 ng/mL, Sigma-Aldrich, P1585) and Ionomycin (1 μg/mL, Sigma-Aldrich, IO634-1MG) in the presence of 1× Brefeldin A (Thermo Fisher Scientific, 00-4506-51) for 4 hours in complete media at 37°C prior to staining.

Flow cytometry fluorescent dye–conjugated antibodies specific for the following proteins were purchased from BioLegend: CD8α APC, clone 53-67; CD4 BV650, clone RM4-5; CD3 AF700, clone 17A2; CD45 BV605, clone 30-F11; CD49b APC/Cy7, clone DX5; CD25 BV421, clone PC61; CD25 APC/Fire 750, clone PC61; Ki67 PeCy7, clone 16A8; Ki67 AF700, clone 16A8; granzyme B FITC, clone GB11; IFNγ PE, clone XMG1.2; F4/80 Pe/Dazzle 594, clone BM8; CD3 Complex PeCy7, clone 17A2; FC Block, clone 93. Flow cytometry fluorescent dye–conjugated antibodies specific for the following proteins were purchased from eBioscience: CD45 BUV395, clon30-F11; CD4 BUV496, clone GK1.5; CD8 BUV563, 53.6–7; TNF BV750, clone MP6-XT22; CD49B Pe-Cy5, clone DX5, FoxP3 AF488, clone FJK-16s; FoxP3 eFlour450, clone FJK-16s. The fluorescent dye–conjugated tetramer against the MulV p15E peptide KSPWFTTL was purchased from Thermo Fisher Scientific (50-168-9385). The Live/Dead Blue Dye was also purchased from Thermo Fisher Scientific (L23105).

Ex vivo INDUKINE protein processing assay

Primary human healthy cells were purchased from either ATCC, Lonza, or Zen-Bio, and cultured according to the manufacturers' protocols. Dissociated human tumor samples were purchased from Discovery Life Sciences and included samples from the following indications: bladder cancer, breast cancer, cervical cancer, colorectal cancer, endometrial cancer, gastric cancer, head and neck cancer, kidney cancer, melanoma, and non–small cell lung cancer (adenocarcinoma and squamous). These samples are generated from primary human tumor samples that were surgically removed and enzymatically digested on site prior to being frozen. All purchased samples were shipped to Werewolf Therapeutics on dry ice and were stored in a liquid nitrogen freezer.

To examine INDUKINE protein processing, samples were thawed, washed, and counted. Cells were then resuspended in media containing either intact WTX-124, WTX-124-NC, or precut WTX-124. INDUKINE proteins were incubated with cells for 48 hours before cell culture supernatants were collected and frozen for later analysis. The IL-2 Bioassay, which utilizes thaw-and-use IL-2 reporter cells, was used to assess the amount of free IL-2 in the cell culture supernatants (Promega, JA2201/JA2205). This bioassay was used according to the manufacturer's protocol and analyzed using a Perkin Elmer Enspire reader and Enspire Manager Software (V4.13.3005.1482). Relative luminescence unit (RLU) values were translated into percent full activity using the following equation:

$$Percent\ of\ Full\ Activity = \left(1 - \frac{(Sample\ -\ Uncleavavble\ Ctrl)}{(Cleaved\ Ctrl - Uncleavable\ Ctrl)}\right) * 100$$

Data representation and statistical analysis

For murine tumor experiments, mice were implanted with the respective tumor cell lines such that each group had at least $n = 8$ mice per group at the time of randomization and the initiation of dosing. To have sufficient animals to appropriately randomize based on tumor size, the total number of mice implanted was calculated by adding 30% to the total number of animals needed on study. Sample size was determined by previous experience with this model, and tumor measurements were made in an unblinded fashion. Flow cytometry plots were generated with FlowJo Software (v10.5.30) and are representative samples. All the quantitative plots were generated using GraphPad Prism 8 Software for Windows (64-Bit). For *in vitro* activity assays, data were analyzed using a nonlinear sigmoidal, 4PL curve fit model without constraints. Statistical analysis was also performed using GraphPad Prism software. Two sample comparisons used a Student *t* test while comparisons of more than two groups used an ANOVA test with multiple comparisons. Antitumor effects over time were analyzed by using a mixed-effects model. For the NanoString dataset, statistical analysis was performed using nSolver software with the Advanced Analysis Module installed.

Data availability

The NanoString data generated in this study are available upon reasonable request from the corresponding author with appropriate legal agreements in place. Other data generated in this study are available within the article and its Supplementary Data files.

Results

WTX-124 signaling and activity is dependent on proteolytic activation

WTX-124, an IL-2 containing INDUKINE protein, was designed to enhance the clinical profile of rhIL-2 treatment by facilitating less frequent systemic delivery, increasing the tumor exposure of the molecule, and decreasing the toxicity associated with high-dose IL-2. WTX-124 includes native human IL-2, a Fab antibody fragment that prevents IL-2 from binding to the medium-affinity IL-2 receptor (IL-2Rβ/γ), thereby acting as an inactivation domain, and an anti-human serum albumin single-domain antibody, which acts as a half-life extension domain (**Fig. 1A**). These two domains are linked to the IL-2 payload via a protease-cleavable linker sequence. WTX-124 in the prodrug state is half-life extended, and the activity of IL-2 is inhibited because the binding of the molecule to the IL-2 receptors is blocked by the Fab antibody fragment. When the linkers are enzymatically cleaved in tumor tissue, the half-life extension and inactivation domains are removed, and native IL-2 is released (**Fig. 1B**).

To measure the difference in activity between intact and protease-cleaved WTX-124, HEK-Blue IL-2 reporter cells were incubated with either rhIL-2, intact WTX-124, or protease-activated (cleaved) WTX-124 and then IL-2 signaling was measured. In this assay, intact

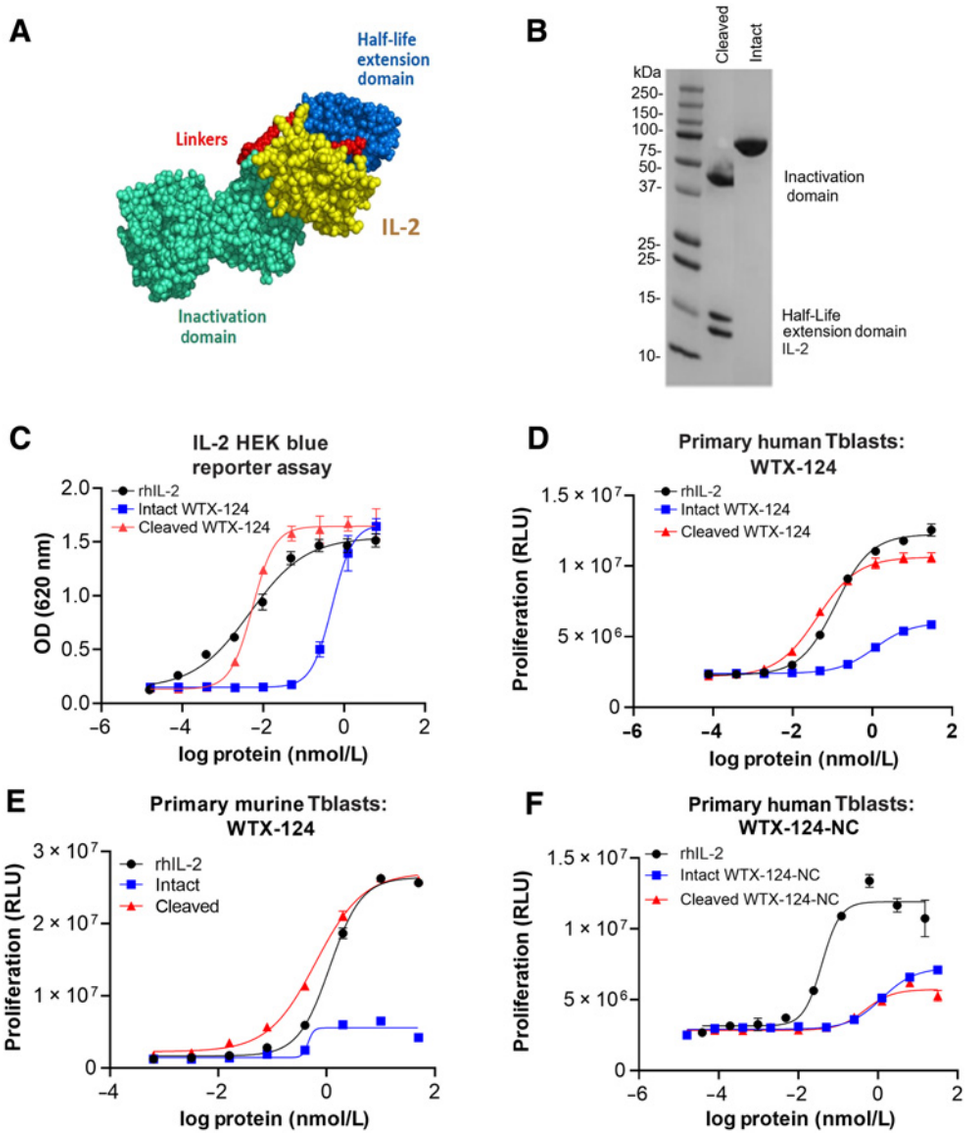

Figure 1.

Design and development of the selectively active IL-2 INDUKINE protein WTX-124. **A,** Diagram of the components of WTX-124. The yellow section represents IL-2, the blue section represents the half-life extending HSA-specific single-domain antibody, the teal section represents the activity blocking Fab, and the red sections represent the protease-cleavable linkers. **B,** Nonreduced SDS-PAGE comparing intact and protease-cleaved WTX-124 (IL-2, anti-HSA half-life extension domain, and the Fab inactivation domain). **C,** *In vitro* activity of WTX-124 in the HEK-Blue IL-2 reporter assay comparing intact (blue), and protease-activated (cleaved) WTX-124 (red) to rhIL-2 (black). *In vitro* activity of intact (blue) and cleaved (red) WTX-124 in primary human (**D**) or murine (**E**) Tblasts compared with rhIL-2 (black). **F,** *In vitro* activity of intact (blue) and "cleaved" (red) WTX-124-NC in primary human Tblasts compared with rhIL-2 (black). **C–F,** Curves are representative of at least duplicate wells and depict the mean ± SD for individual points; data are representative of at least two experiments. HEK, human embryonic kidney; HSA, human serum albumin; OD, optical density; RLU, relative luminescence units.

WTX-124 had approximately 100-fold less activity than either rhIL-2 or cleaved WTX-124 (**Fig. 1C**). Additionally, human PBMCs were stimulated with PHA to form Tblasts, which express the high-affinity IL-2 receptor (CD25/CD122/CD132; Supplementary Fig. S1A and S1B) and respond to IL-2 signaling by proliferating. Human Tblasts from multiple donors were exposed to rhIL-2, intact WTX-124, or cleaved WTX-124 for 72 hours and then Tblast proliferation was measured. In this system, intact WTX-124 had less activity than either cleaved WTX-124 or rhIL-2 across multiple donors (**Fig. 1D**; Supplementary Fig. S1C). More specifically, intact WTX-124 had approximately 23-fold less activity in terms of an increased half maximal effective concentration (EC_{50}) and plateaued at only approximately 40% of the maximum activity seen with either cleaved WTX-124 or rhIL-2.

The activity of intact and cleaved WTX-124 was also characterized in a mouse primary Tblast assay. Although cleaved WTX-124 and rhIL-2 induced similar proliferation by murine Tblasts, intact WTX-124 had almost no measurable activity in cells isolated from

multiple mice (**Fig. 1E**; Supplementary Fig. S1D). To confirm that the activity of cleaved WTX-124 was dependent on linker cleavage and not an unknown processing event, a noncleavable variant of WTX-124 (WTX-124-NC) was generated by replacing the linker sequence with a noncleavable glycine/serine sequence. As a control, WTX-124-NC was treated to the same enzymatic digestion as WTX-124 before being tested in human Tblasts. No difference in activity was seen between the intact and "cleaved" forms of WTX-124-NC, demonstrating the necessity of linker cleavage for fully active IL-2 to be released from the WTX-124 prodrug (**Fig. 1F**).

WTX-124 treatment controls tumor growth in a cleavage-dependent manner and prevents the toxicity associated with systemic IL-2 administration

To test whether WTX-124 treatment could inhibit tumor growth, mice were implanted with MC38 tumor cells and randomized into treatment groups when the tumors were between 100 and 150 mm^3. Mice were then treated twice a week with vehicle (PBS) or titrated amounts of WTX-124 for a total of four doses. In this model, even the lowest dose of WTX-124 (25 μg) resulted in statistically significant tumor growth inhibition (**Fig 2A** and **B**; Supplementary Fig. S2A). Furthermore, doses of 100, 150, or 300 μg were all highly efficacious. Of the 24 mice in those dosing groups, 23 had complete responses with no measurable tumor remaining at the end of the study (**Fig. 2A**; Supplementary Fig. S2A). All dose levels were well tolerated by the mice, with no signs of body weight loss (Supplementary Fig. S2B). In addition, some mice were dosed with a variant of WTX-124 that did not contain the half-life extension domain (WW0057). This molecule failed to generate antitumor immunity, even when given at 10-fold the fully efficacious dose of the parent INDUKINE molecule (Supplementary Fig. S2C). To confirm that the *in vivo* processing of the protease cleavable linkers was critical for the activity of WTX-124, some MC38 tumor-bearing mice were dosed with WTX-124-NC. Because WTX-124 retains some residual activity when tested at a high concentration *in vitro* (**Fig. 1C–E**), WTX-124-NC acts as a control for the level of *in vivo* activity derived specifically from intact WTX-124, and not from the proteolytic processing and subsequent release of fully active IL-2. In contrast to WTX-124, even when WTX-124-NC was administered at the highest tested dose (300 μg), it had limited effects on tumor growth, and none of the treated animals had complete responses (**Fig. 2A**). These data demonstrate that the antitumor activity of WTX-124 is dependent on *in vivo* enzymatic cleavage of its linkers.

To assess how well the inactivation domain of WTX-124 prevented the toxicity derived from signaling in peripheral (nontumor) tissues, an unblocked variant of WTX-124 was created. WW0177 differs from WTX-124 in that it contains a noncleavable linker sequence between the half-life extension domain and the fully active IL-2, and it does not have an inactivation domain, thereby representing the level of toxicity that should be expected if the inactivation domain of WTX-124 was not functioning properly. MC38 tumor-bearing mice were dosed with either WW0177 or WTX-124, and their weight was monitored over time (**Fig. 2C**). After only two doses of WW0177, dosing had to be halted because of body weight loss, and only 2 of 7 mice survived. In contrast, mice treated with four doses of WTX-124 had no evidence of weight loss, despite being given approximately 26 times the molar amount of IL-2 that was administered to the group receiving WW0177. Although weight loss is a useful surrogate to monitor overall toxicity in regard to immunotherapies, it was also important to investigate the effects of IL-2 INDUKINE molecules on known organ-specific toxicity associated with IL-2 in the clinic. VLS is a major dose-limiting toxicity associated with high-dose IL-2 treatment and is defined as an increase in vascular permeability that leads to the extravasation of fluids and eventual organ failure in patients. In mice, VLS can be assessed by measuring the amount of Evan's Blue dye that leaks into the lungs following intravenous administration of the dye. In agreement with the overall toxicity data, when rhIL-2, WW0177, or the IL-2 INDUKINE protein were administered in equimolar amounts, only rhIL-2 and WW0177 resulted in detectable levels of Evans Blue leaking into the lungs; the IL-2 INDUKINE molecule did not (Supplementary Fig. S2D). Together, these data demonstrate that the inactivation domain of WTX-124 effectively blocks the activity of IL-2 in nontumor tissues and prevents the induction of VLS compared with permanently active IL-2 molecules.

Although the inactivation domain of WTX-124 is highly effective, the efficiency of this domain is dependent on the blocker remaining linked to the IL-2 molecule (**Fig. 1**). To examine the stability of WTX-124 in the periphery, WTX-124 was incubated in murine plasma from either naïve or MC38 tumor-bearing mice for 24, 48, or 72 hours before the level of intact WTX-124 was measured by Western blot analysis. In agreement with the tolerability of the molecule, there was no evidence of WTX-124 cleavage across all tested timepoints (**Fig. 2D**).

In addition to managing peripheral toxicity, WTX-124 was designed to facilitate less frequent, systemic delivery of the treatment without sacrificing the antitumor activity of high-dose IL-2. Therefore, it was important to directly compare the activity of WTX-124 with native IL-2. MC38 tumor-bearing mice were treated with titrated amounts of either WTX-124 as before (twice weekly for 2 weeks) or rhIL-2 dosed twice a day for 2 weeks (dosing regimen: 5 days dosing, 2 days rest repeated for 2 weeks). The differences in the dosing schedules reflect the poor *in vivo* pharmacokinetic properties of rhIL-2 in both humans (14) and mice (15) and mimic the dosing of patients with high-dose IL-2 in the clinic. Because the two treatments are delivered on different dosing regimens, the treatment groups were compared using the total amount of IL-2 delivered during the dosing period. MC38 tumor-bearing mice treated with a total of 5.04 μmol of WTX-124 resulted in 8 of 8 mice showing complete tumor rejection. In contrast, treatment with 15.5 μmol of native IL-2 (three times the total amount of IL-2 dosed with WTX-124) had only 5 of 8 mice completely rejecting the tumors (**Fig. 2E**).

As noted previously, the poor pharmacokinetic profile [half-life ($t_{1/2}$) < 1 hour] of proleukin treatment results in an impractical dosing regimen, with many patients receiving a high dose every 8 hours for up to 15 doses (16). Likewise, in mice, rhIL-2 is rapidly cleared from circulation (15). We hypothesized that the increased activity of WTX-124 compared with native IL-2 is due to its extended half-life and improved pharmacokinetic profile. To confirm this, MC38 tumor-bearing mice were dosed once on day 0 and once on day 4, and the drug exposure was measured in the plasma and within the tumor at various timepoints. In contrast to rhIL-2, WTX-124 dosing resulted in extended exposure in the plasma, with a half-life of approximately 20 hours, and exposure maintained over the course of 4 days (**Fig. 2F**). In addition, intraperitoneal dosing of WTX-124 resulted in prolonged drug exposure within the tumor itself, demonstrating tissue penetrance by WTX-124 (**Fig. 2G**). Total WTX-124 levels reached a peak concentration (C_{max}) at 6 hours postdosing in the plasma and 12 hours postdosing in the tumor.

To examine whether systemic dosing of WTX-124 resulted in localized delivery of human IL-2 into the tumor, plasma and tumor samples were collected at various timepoints after dosing and were analyzed for the presence of free human IL-2 (i.e., not bound to the

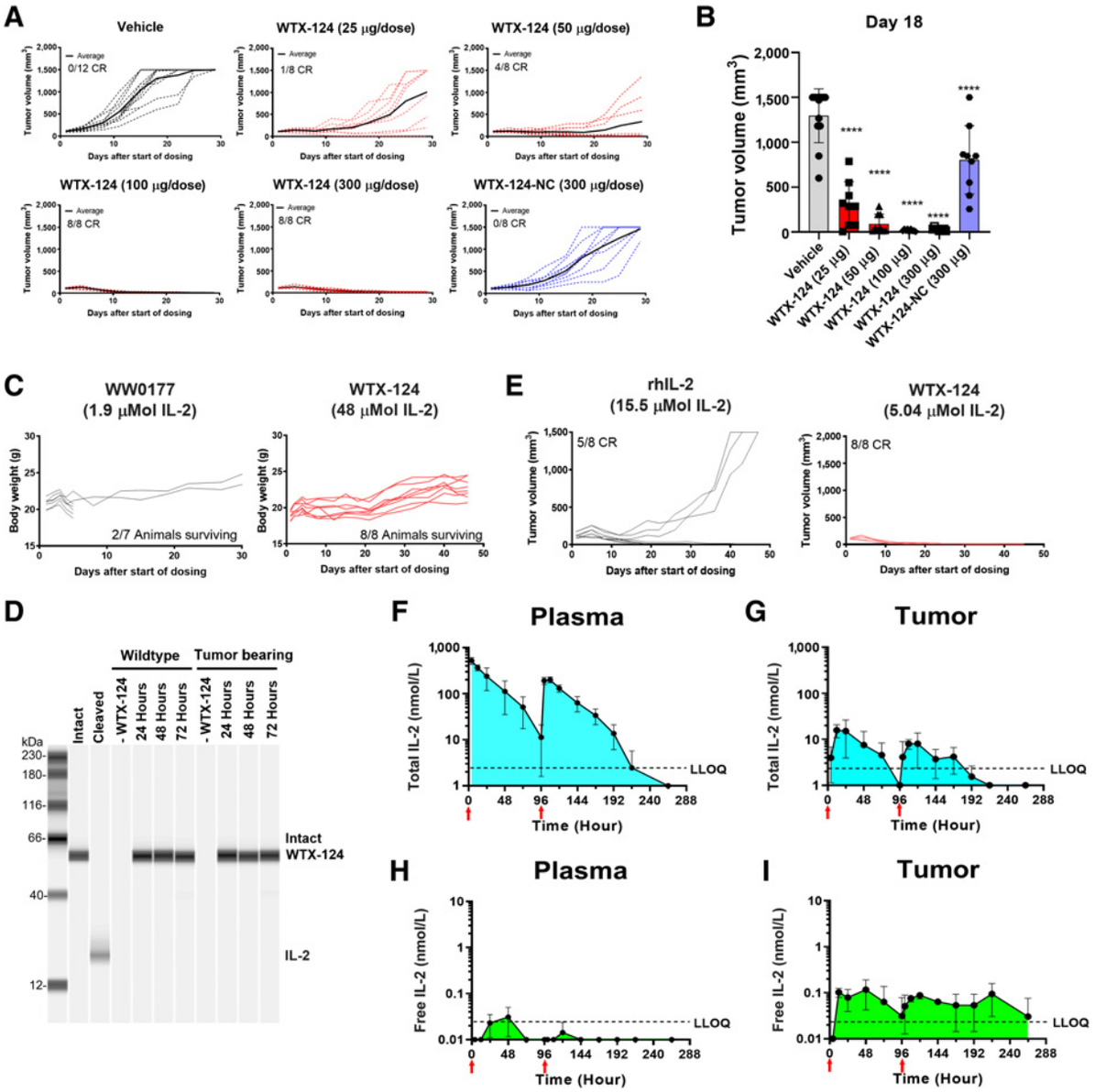

Figure 2.

WTX-124 treatment induces tumor regression in a cleavage-dependent manner. MC38 tumor cells were implanted and allowed to grow to an average volume of 100–150 mm^3 before mice were randomized into treatment groups. Mice were dosed twice a week with INDUKINE proteins, or twice a day for 5 days followed by 2 rest days with rhIL-2. Mice were dosed for 2 weeks unless otherwise noted. **A,** Mice were treated with either various doses of WTX-124, WTX-124-NC (noncleavable control), or vehicle, and tumor volume was measured over time. Spider plots for individual mice are reported (dashed lines), and the average tumor volume for the group is in bold. **B,** Tumor volume on day 18. **C,** Mice were treated with either WTX-124 or WW0177 (a WTX-124 variant lacking the inactivation domain). Body weight and survival from individual mice over time is shown. Dosing of WW0177 was halted after two doses due to excessive toxicity, whereas mice receiving WTX-124 were given all four doses. **D,** WTX-124 was diluted in murine plasma from either wild-type or MC38 tumor-bearing mice and incubated at 37°C for 24, 48, or 72 hours before WTX-124 processing was measured by Western blot analysis for IL-2. Intact and cleaved controls were prepared *in vitro.* Data are representative of $n = 3$ mice. **E,** Mice were treated with efficacious amounts of either WTX-124 (5.04 μmol total) or rhIL-2 (15.5 μmol total), and tumor volume was measured over time. Spider plots for individual mice are reported. Plasma (**F** and **H**) and tumor (**G** and **I**) samples from tumor-bearing mice were analyzed at various timepoints for either the presence of the total INDUKINE protein (**F** and **G**) using an ELISA that detects both intact WTX-124 as well as free IL-2, or free human IL-2 (**H** and **I**) using an AlphaLISA specific for unblocked human IL-2. Mice received only two doses, and the timing of the doses is indicated by the red arrows on the figure. **F–I,** Data are presented as the mean ± SD, and AUC measurements were calculated using GraphPad Prism software. *P* values are derived from a one-way ANOVA followed by Dunnett multiple comparisons comparing each sample with the vehicle control (****, $P < 0.0001$). ANOVA, analysis of variance; LLOQ, lower limit of quantification; MC, murine colon.

inactivation domain) released because of the enzymatic processing. To specifically measure human IL-2 released from the INDUKINE construct by proteolytic processing, we identified an ELISA kit that was specific for human IL-2 (Supplementary Fig. S2E), where the inactivation domain of WTX-124 prevented the binding of the ELISA detection reagents (Supplementary Fig. S2F). This allowed us to assess the level of free, human IL-2 present in the tumor and in the plasma, which could only be generated by the *in vivo* processing of WTX-124. Systemic dosing with WTX-124 resulted in almost no detectable free human IL-2 in the plasma (**Fig. 2H**). In contrast, systemic dosing with WTX-124 resulted in prolonged levels of detectable free human IL-2 in the tumor (**Fig. 2I**), demonstrating that tumor-dependent processing continually releases fully active IL-2 in the tumor following systemic WTX-124 delivery.

To better quantify the differences between plasma and tumor in terms of WTX-124 processing, the area under the exposure curves was measured (**Fig. 2F–I**; Supplementary Table S1). Although the amount of total WTX-124 in the plasma was about 18-fold greater than in the tumor, the amount of free IL-2 in the tumor was still over 5-fold greater than that detected in the plasma, which suggests an approximately 93-fold increase in INDUKINE protein processing in the tumor compared with the plasma.

The therapeutic window (TW) of a treatment is defined as the ratio of the maximum tolerated dose (MTD) and the minimum efficacious dose (MED), thereby measuring the distance between clinical activity and serious adverse events. In the clinic, the TW for proleukin is relatively small. Similarly, the TW of rhIL-2 in MC38 tumor-bearing mice was calculated to be less than 4-fold in our model (Supplementary Fig. S2G). By comparison, since the half-life extension element of WW0177 resulted in greater IL-2 exposure *in vivo*, less WW0177 was required to reach full efficacy compared with rhIL-2. However, due to its permanently active state, WW0177 also has a lower MTD, resulting in a TW similar to that of rhIL-2 (<2, Supplementary Fig. S2G). In contrast, the engineering of WTX-124 resulted in significantly greater activity than equimolar amounts of rhIL-2 (**Fig. 2E**) and allowed for selective activation in the TME, thereby preventing the toxicity associated with exposure to half-life extended IL-2 molecules (**Fig. 2C**). Indeed, no toxicity was seen in MC38 tumor-bearing mice dosed with up to 960 μg/dose of WTX-124, resulting in the TW of WTX-124 in this model being greater than 20 at a minimum, representing at least a 5-fold improvement over rhIL-2 (Supplementary Fig. S2G). These data demonstrate that WTX-124 is not simply a half-life extended, attenuated IL-2 molecule, but instead a unique, selectively inducible IL-2 prodrug that enhances the activity of the payload while restricting its systemic activity.

WTX-124 treatment of MC38 tumor-bearing mice results in immunologic memory

One hallmark of immunologic rejection of a tumor is the development of protective memory against subsequent tumor rechallenge. To test whether WTX-124 treatment resulted in tumor-specific memory following tumor rejection, mice were implanted with MC38 tumor cells and randomized into vehicle or WTX-124 treatment groups, and tumor growth was measured. As with previous studies, WTX-124 treatment resulted in tumor rejection, whereas the control tumors continued to grow. To examine whether tumor rejection in WTX-124–treated mice resulted in immunologic memory, spleens from mice were examined for the presence of tumor-specific memory $CD8^+$ T cells 6 months after the initial MC38 implantation (MC38 CR mice; **Fig. 3A**). Previous studies have identified that a peptide derived from Murine Leukemia Virus envelope protein (KSPWFTTL) is an antigen presented by MC38 tumors and that T cells specific for this antigen can be identified using fluorescently labeled MHC–peptide complexes known as tetramers (17). Spleens from MC38 CR mice had a higher overall frequency of tetramer-positive $CD8^+$ T cells than age-matched tumor-naïve mice (**Fig. 3A** and **B**). Furthermore, although the tetramer-positive cells from tumor-naïve mice largely maintained a naïve phenotype, cells from MC38 CR mice were predominantly of an effector memory phenotype ($CD44^{hi}CD62L^{low}$; **Fig. 3C** and **D**). Upon restimulation, tetramer-positive cells from MC38 CR mice secreted more of the effector cytokines TNF and IFNγ (**Fig. 3E** and **F**). Coexpression of two or more effector cytokines is known as polyfunctionality, and it is associated with greater cytolytic activity in T cells (18, 19). WTX-124–induced MC38 CR mice also had a significantly increased frequency of polyfunctional tetramer-positive $CD8^+$ T cells following restimulation (**Fig. 3G**). These data are consistent with the idea that WTX-124 treatment results in immune-mediated tumor rejection which then translates into immunologic memory.

Nevertheless, the ultimate test of a memory response is protection against rechallenge. Therefore, IL-2 INDUKINE-induced MC38 CR mice were rechallenged with MC38 tumor cells 60 days after the initial implantation (**Fig. 3H**). No treatment was administered during the rechallenge. Unlike the tumor-naïve mice, none of the MC38 CR mice developed tumors (**Fig. 3I**), demonstrating that WTX-124–induced tumor rejection results in immunologic memory and protection against subsequent tumor rechallenge.

WTX-124 treatment amplifies MC38 tumor infiltration and induces immune cell activation

To better understand the mechanism by which WTX-124 treatment induces antitumor immunity, MC38 tumor-bearing mice were randomized into treatment groups on day 0 and treated with either vehicle or WTX-124 on day 1 and day 4. Tumors were harvested 24 hours after the second dose. Total RNA was extracted from the single-cell suspensions and analyzed using the NanoString nCounter PanCancer Mouse Immune Profiling Panel. WTX-124 treatment resulted in a clear shift in the transcriptional profile, with 437 of 770 genes in the panel having statistically significant differences in expression compared with the control group (**Fig. 4A** and **B**). NanoString nSolver pathway analysis of this dataset revealed a series of immune activation–related pathways that were upregulated by WTX-124 treatment, including both broad immune activation signatures such as adaptive immunity and inflammation, as well as more specific signatures such as leukocyte function, NK-cell function, and T-cell function (**Fig. 4C**). The expression of several transcripts associated with immune checkpoint proteins also increased following WTX-124 treatment, including PD-1, TIGIT, and CTLA-4 (**Fig. 4D**). This likely reflects the overall increase in immune cell activation among the tumor-infiltrating lymphocytes (TIL), as many checkpoint proteins are upregulated during a typical immune response.

In addition to the NanoString analysis, immune cell profiling by flow cytometry was also performed, using the gating strategy found in Supplementary Fig. S3A. As soon as 5 days after the initial dose, WTX-124 treatment resulted in a large increase in the density of infiltrating immune cells, including tumor-specific tetramer-positive $CD8^+$ T cells (∼19.8-fold increase) and to a lesser extent Tregs (∼2.5-fold increase; **Fig. 4E**). Therefore, although intratumoral Tregs did expand in response to the local release of native IL-2 from the processing of WTX-124, the expansion of the tumor-infiltrating, tetramer-positive $CD8^+$ T cells was much larger, resulting in a significant increase in the tetramer-positive $CD8^+$/Treg ratio after WTX-124 treatment (**Fig. 4F**).

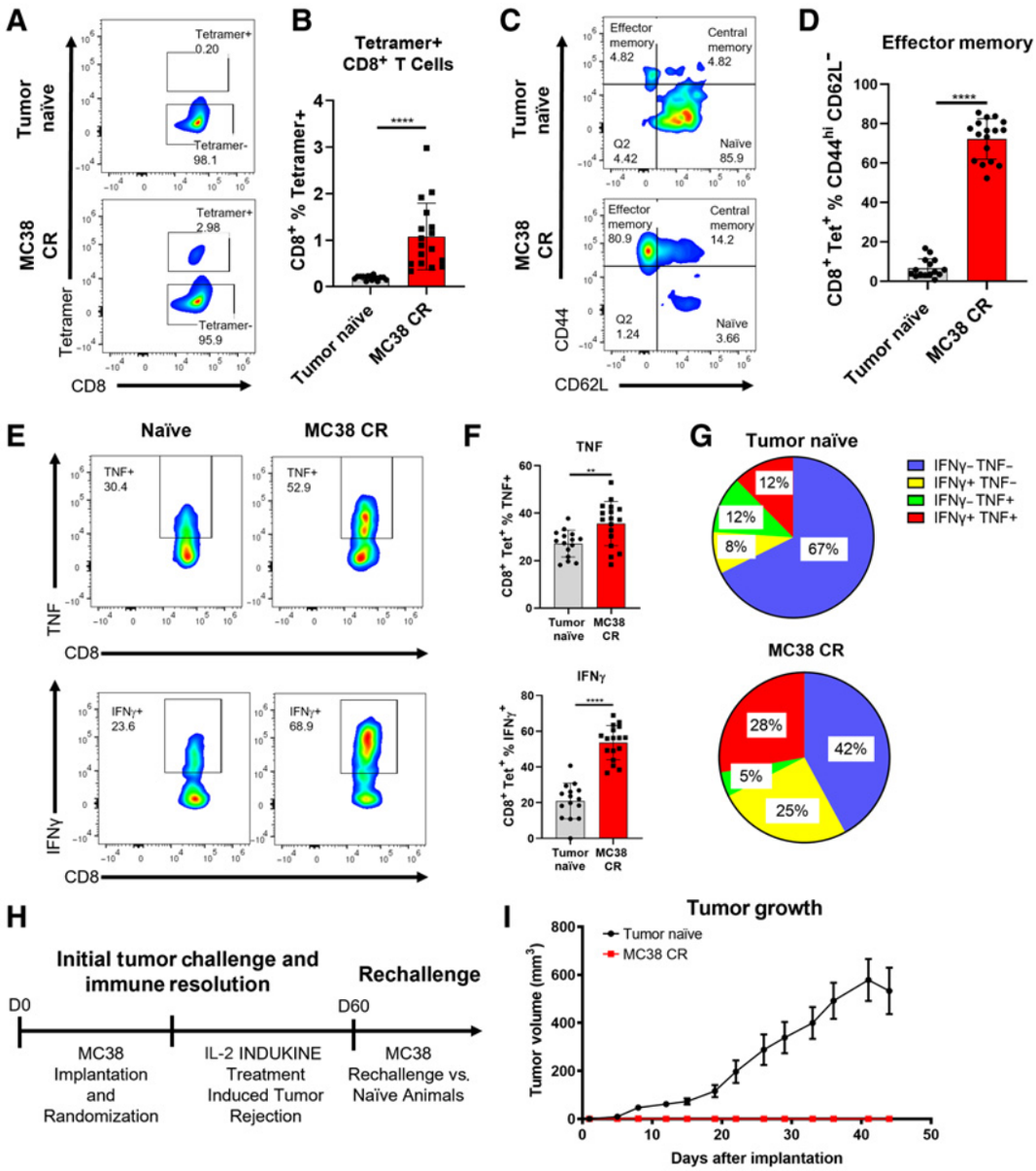

Figure 3.

WTX-124 treatment induces an antitumor memory response. MC38 tumor cells were implanted and allowed to grow to an average volume of 100–150 mm^3 before mice were randomized into treatment groups. Mice were dosed twice a week with varying doses of WTX-124 (50–300 μg/dose) for a total of four treatments (**Fig. 2A**). Spleens from any mice that rejected the MC38 tumors (MC38 CR) were examined 6 months after the initial implantation and compared to age-matched, tumor-naïve mice. Splenocytes were assessed for the frequency of tetramer-positive $CD8^+$ T cells (**A** and **B**) and the expression of the memory cell markers CD62L and CD44 on tetramer-positive $CD8^+$ T cells (**C** and **D**), as well as for the frequency of tetramer-positive $CD8^+$ T cells producing TNF or IFNγ (**E** and **F**). **G,** Analysis of polyfunctional tetramer-positive $CD8^+$ T cells coexpressing IFNγ and TNF. **H** and **I,** Naïve mice or mice that had previously rejected MC38 tumors after IL-2 INDUKINE treatment were rechallenged with MC38 tumor cells 60 days following the initial implantation. No treatment was administered to these mice during the rechallenge. **I,** Tumor volume from MC38 CR ($n = 15$) or naïve ($n = 33$) mice was measured over time and is represented as the mean ± SEM. Remaining data are presented as mean ± SD for quantification plots, with P values derived from t tests (**, $P < 0.01$; ****, $P < 0.0001$).

To assess the activation state of the tumor-infiltrating T cells, samples from the TILS were restimulated, and the production of IFNγ, TNF, and granzyme B was assessed. WTX-124 treatment significantly increased the frequency of tetramer-positive $CD8^+$ T cells producing IFNγ (**Fig. 4G** and **H**), TNF (Supplementary Fig. S3B), and granzyme B (Supplementary Fig. S3C). WTX-124 treatment also significantly increased the polyfunctionality of the tumor-infiltrating tetramer-positive $CD8^+$ T cells, with over 60% of the cells from WTX-124–treated animals producing either two or all three of these effector cytokines compared with only 23% in the control group (**Fig. 4I**).

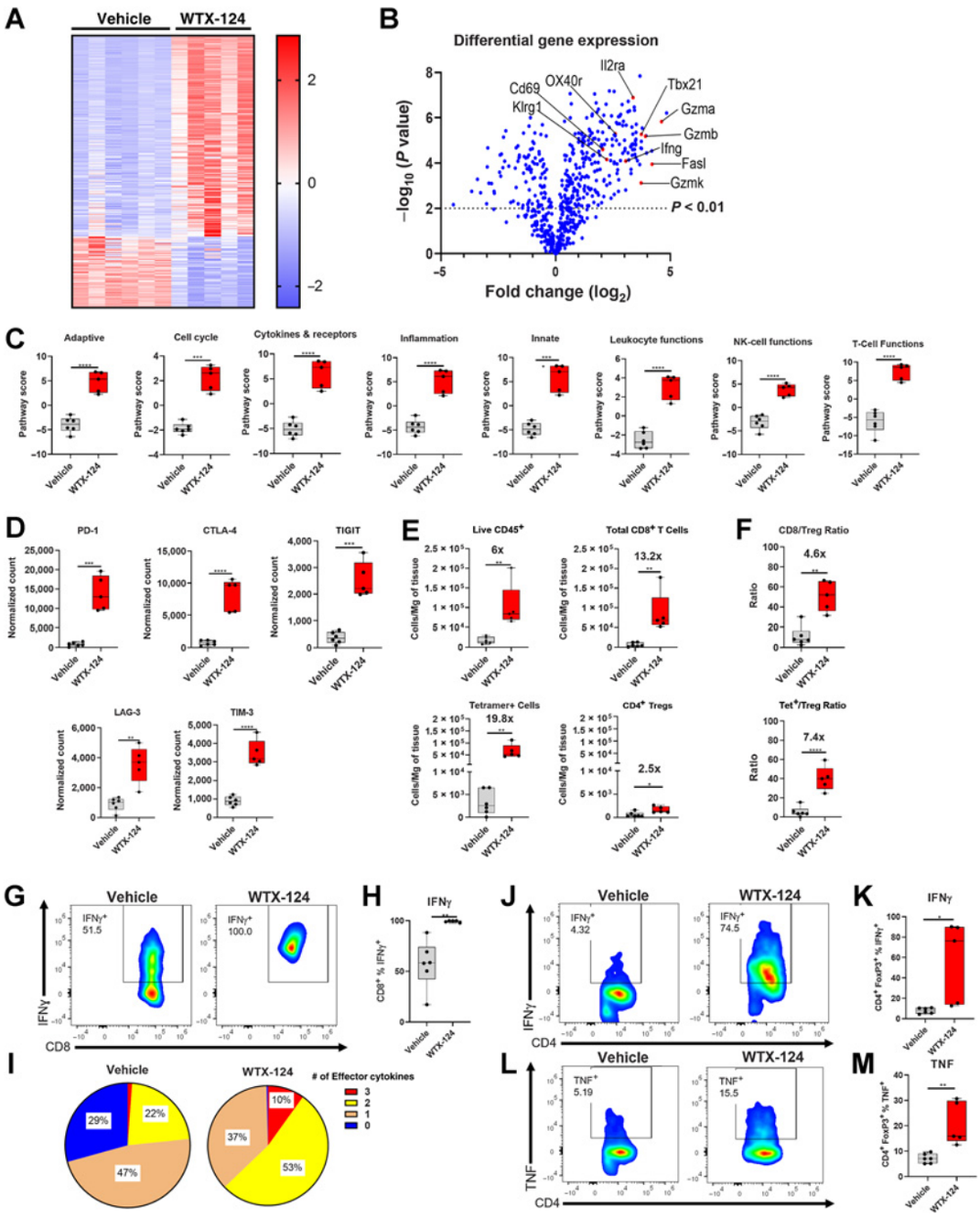

Figure 4.

WTX-124 treatment increases immune cell activation and infiltration of MC38 tumors. MC38 tumor cells were implanted and allowed to grow to an average volume of 100–150 mm^3 before mice were randomized into treatment groups. Mice were dosed twice a week with WTX-124 (100 μg) or PBS. Tumors were collected 24 hours after the second dose and dissociated for further analysis. **A** and **B,** RNA from each tumor was isolated and subjected to immune profiling with the NanoString PanCancer Mouse Immune Profiling Panel. **A,** Heatmap of transcripts with statistically significant differences in expression between the two treatments. Transcripts were excluded from the heatmap if they had average normalized counts below 50. Each lane represents an individual animal. **B,** Volcano plot of transcripts differentially expressed between WTX-124 and vehicle-treated mice. **C,** Specific pathway scores for WTX-124 or vehicle-treated mice. *P* values are derived from a two-way ANOVA with multiple comparisons (***, $P < 0.001$; ****, $P < 0.0001$). **D,** Normalized gene counts from selected immune checkpoint genes. **E,** Flow cytometry analysis of TIL density of various immune populations, including fold change information between the vehicle-treated and WTX-124–treated groups. **F,** The ratio of total $CD8^+$ T cells or tetramer-positive $CD8^+$ T cells to Tregs within the TILs, including fold change information between the vehicle and WTX-124–treated groups. **G** and **H,** The frequency of tetramer-positive $CD8^+$ T cells producing IFNγ after restimulation with PMA/Ionomycin. **I,** The frequency of polyfunctional tetramer-positive $CD8^+$ T cells by examining coexpression of IFNγ, TNF, and granzyme B after PMA/Ionomycin restimulation. The frequency tumor infiltrating $FoxP3^+$ Tregs producing IFNγ (**J** and **K**) or TNF (**L** and **M**) after PMA/Ionomycin restimulation. Unless otherwise stated, data are presented as the mean ± SD, and *P* values are derived from *t* tests (*, $P < 0.05$; **, $P < 0.01$; ***, $P < 0.001$; ****, $P < 0.0001$). CTLA-4, CTL-associated protein 4; LAG-3, lymphocyte-activation gene 3; Tet, tetramer; TIGIT, T-cell immunoglobulin and ITIM (immunoreceptor tyrosine-based inhibitory motif) domain; TIM-3, T-cell immunoglobulin and mucin domain-containing protein 3.

Recent data have demonstrated that under certain circumstances, Tregs can also produce effector cytokines such as TNF and IFNγ, in a phenomenon known as "Treg Fragility" (20). The production of effector cytokines by Tregs is associated with the loss of their suppressive activity. We found that although very few Tregs from the control tumors produced either IFNγ or TNF, a subpopulation of Tregs from the WTX-124–treated tumors produced both of these effector cytokines (**Fig. 4J–M**). Together, these data demonstrate that WTX-124 treatment increases tumor infiltration, activates tumor-specific $CD8^+$ T cells, and causes phenotypic instability of Tregs.

Tumor-specific activation of immune cells by WTX-124 is sufficient to generate tumor rejection

To confirm that the effects of systemic WTX-124 treatment are selective for the TME, effector cytokine production by T cells derived from the tumor, spleen, peripheral blood, and draining lymph nodes were compared after WTX-124 treatment, using the same treatment schedule as described previously. Because the tetramer-positive population is selectively enriched among $CD8^+$ T cells within the tumor, the inclusion of these cells in the analysis could bias the comparison across different sites. Therefore, tetramer-negative $CD8^+$ T cells were specifically examined across the various tissues. As with the previous data, WTX-124 induced a significantly higher frequency of IFNγ-producing $CD8^+$ T cells and $CD4^+$ non-Tregs within the tumor, compared with relatively minor levels of activity seen in the examined peripheral tissues (**Fig. 5A** and **B**). Together with the earlier toxicity data, these data demonstrate that WTX-124 treatment does not result in widespread, peripheral T-cell activation.

While the peripheral $CD8^+$ T-cell activation seen with WTX-124 treatment was limited, it remained possible that this low level of peripheral activity was still playing a role in generating the antitumor immunity in this model. To test whether tumor-specific IL-2 activity was sufficient to generate antitumor immunity, mice were implanted with MC38 tumors that grew to around 100 to 150 mm^3 before some mice were treated with FTY720 (Fingolimod). FTY720 is a small molecule that blocks the sphingosine-1-phosphate receptors, thereby preventing lymphocyte egress from the thymus and secondary lymphoid tissues (21). Therefore, any antitumor activity seen in FTY720-treated mice is derived from the immune cells that have already infiltrated the tumor at the start of treatment, and not from the activation and subsequent trafficking of additional lymphocytes from secondary immune tissues. Daily FTY720 treatment had no effect on the antitumor activity of WTX-124 (**Fig. 5C**) demonstrating that tumor-specific delivery of IL-2 alone was sufficient to reject MC38 tumors. Together, these data demonstrate that systemic administration of WTX-124 to tumor-bearing animals results in tumor processing of the INDUKINE molecule and preferential activation of tumor-infiltrating immune cells that is sufficient to generate potent antitumor immunity.

WTX-124 treatment increases immune cell activation in a less immunogenic tumor model

In patients, the presence of a preexisting TIL population, termed a "hot" tumor, correlates with responses to immunotherapy, and the lack of a preexisting TIL population, known as a "cold" tumor, has the opposite correlation. Murine syngeneic tumor models vary in their baseline immune infiltration as well as their responses to immunotherapy. For example, in MC38 tumors, approximately 20% of the TILs are $CD8^+$ T cells compared with only 2.5% in B16-F10 tumors (Supplementary Fig. S4).

To test the activity of WTX-124 in a less immunogenic tumor model, mice were injected subcutaneously with B16-F10 melanoma cells. Tumors were allowed to grow to an average volume of 100 mm^3 before mice were randomized to receive either PBS or various doses of WTX-124, using the same dosing schedule as before. WTX-124 treatment slowed tumor growth in a dose-dependent manner (**Fig. 6A** and **B**; Supplementary Fig. S5A) whereas anti-PD-1 treatment alone was ineffective in this model. Combining the lower dose of WTX-124 with PD-1 blockade demonstrated combinatorial activity. However, no additional benefit of PD-1 blockade was seen with a higher dose of WTX-124.

To further explore the mechanism of tumor growth inhibition, total tumor RNA was extracted from mice treated with WTX-124, 24 hours after the second dose, and analyzed using the NanoString nCounter PanCancer Mouse Immune Profiling Panel. WTX-124 treatment resulted in a large transcriptional shift, with 184 of 770 examined transcripts having a statistically significant difference in expression after WTX-124 treatment (**Fig. 6C**). Immune profiling by flow cytometry of the B16-F10 TILs did not reveal the large increase in immune cells observed in the MC38 tumors after WTX-124 treatment, which may explain the differences in antitumor efficacy between these two models at this dose. However, WTX-124 treatment did induce proliferation and granzyme B production by tumor-infiltrating tetramer-positive $CD8^+$ T cells (**Fig. 6D** and **E**) and NK cells (**Fig. 6F** and **G**). Furthermore, WTX-124 induced greater TIL activation than rhIL-2 in this model, likely due to its increased exposure (Supplementary Fig. S5B and S5C). Finally, just as in the MC38 model, WTX-124 treatment of B16-F10 tumor-bearing mice resulted in a small subset of tumor-infiltrating $FoxP3^+$ Tregs producing inflammatory cytokines such as TNF and IFNγ (**Fig. 6H** and **I**), suggesting that WTX-124 treatment induces Treg fragility in this model as well. Together, these data demonstrate that WTX-124 treatment can induce TIL activation and inhibition of tumor growth in less inflamed, "colder" tumor models.

WTX-124 is stable in human serum and is processed by human tumors

Human tumor samples are heterogeneous in nature and display different degrees of protease dysregulation and expression (11). Therefore, it was important to confirm that WTX-124 was efficiently and selectively processed by a set of primary human tumor samples. As a test of WTX-124 peripheral stability, the protein was incubated with human serum from healthy donors ($n = 3$) for up to 72 hours before processing was measured by Western blot analysis. In agreement with the murine plasma experiments, WTX-124 was not processed by human serum in any of the tested donors (**Fig. 7A**).

To test whether WTX-124 was efficiently processed by human tumor samples, an *ex vivo* processing assay was developed. Briefly, dissociated human tumor samples were incubated with WTX-124 or control proteins for 48 hours before IL-2 activity was measured. Using WTX-124-NC as a proxy for the baseline activity of the intact WTX-124 prodrug, and precut WTX-124 as representative of a fully activated molecule, the activity induced by incubation of WTX-124 with the dissociated human tumor samples was normalized to a range of 0% to 100% activation. In some instances, the primary human tumor samples also contained viable TILs, which have the capacity to consume some of the free IL-2 in the precut WTX-124 positive control group. This may result in the activity of the positive control being artificially depressed in certain samples, which allows for the possibility of some samples recording over 100% activity compared with the positive control. Despite this issue, this assay is sufficient to be

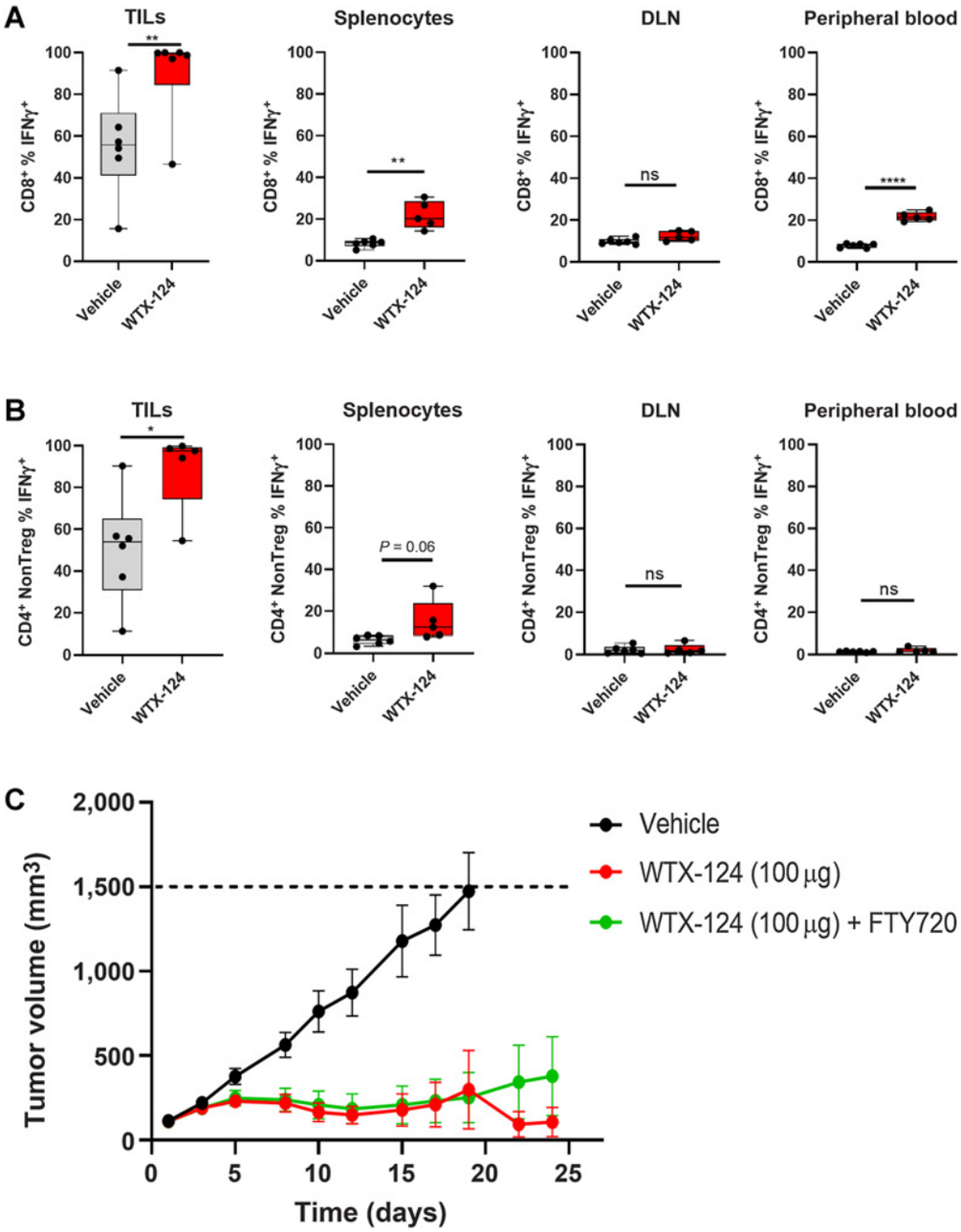

Figure 5.
Systemic WTX-124 treatment preferentially activates tumor-infiltrating T cells. MC38 tumor cells were implanted and allowed to grow to an average volume of 100–150 mm^3 before mice were randomized into treatment groups. Mice were dosed twice a week with WTX-124 (100 μg) or vehicle. Tumors, spleens, DLNs, and peripheral blood samples were collected 24 hours after the second dose. Graphs show the frequency of either tetramer-negative $CD8^+$ T cells (**A**) or $CD4^+$ non-Tregs (**B**) producing IFNγ after restimulation with PMA/Ionomycin. **C,** Mice were treated with either vehicle ($n = 10$), WTX-124 alone ($n = 10$), or WTX-124 with daily FTY720 ($n = 10$) treatment. FTY720 dosing was initiated 24 hours prior to starting WTX-124 treatment (25 μg dose) and maintained daily (10 μg dose) throughout the experiment. Tumor volume (mean ± SEM) was measured over time. Unless otherwise stated, data are presented as the mean ± SD, and *P* values are derived from *t* tests (*, $P < 0.05$; **, $P < 0.01$; ****, $P < 0.0001$). DLN, draining lymph node.

used as a binary analysis of whether or not WTX-124 is being processed by primary human tumor samples. To examine how well WTX-124 was processed by various tissue samples, healthy primary human cells ($n = 13$) and primary human tumor samples ($n = 97$) were examined for the capacity to cleave WTX-124. The healthy primary cells were derived from various tissues, and the tumor samples covered a wide range of tumor types and stages. Importantly, exposure of WTX-124 to the healthy primary cells did not result in any evidence

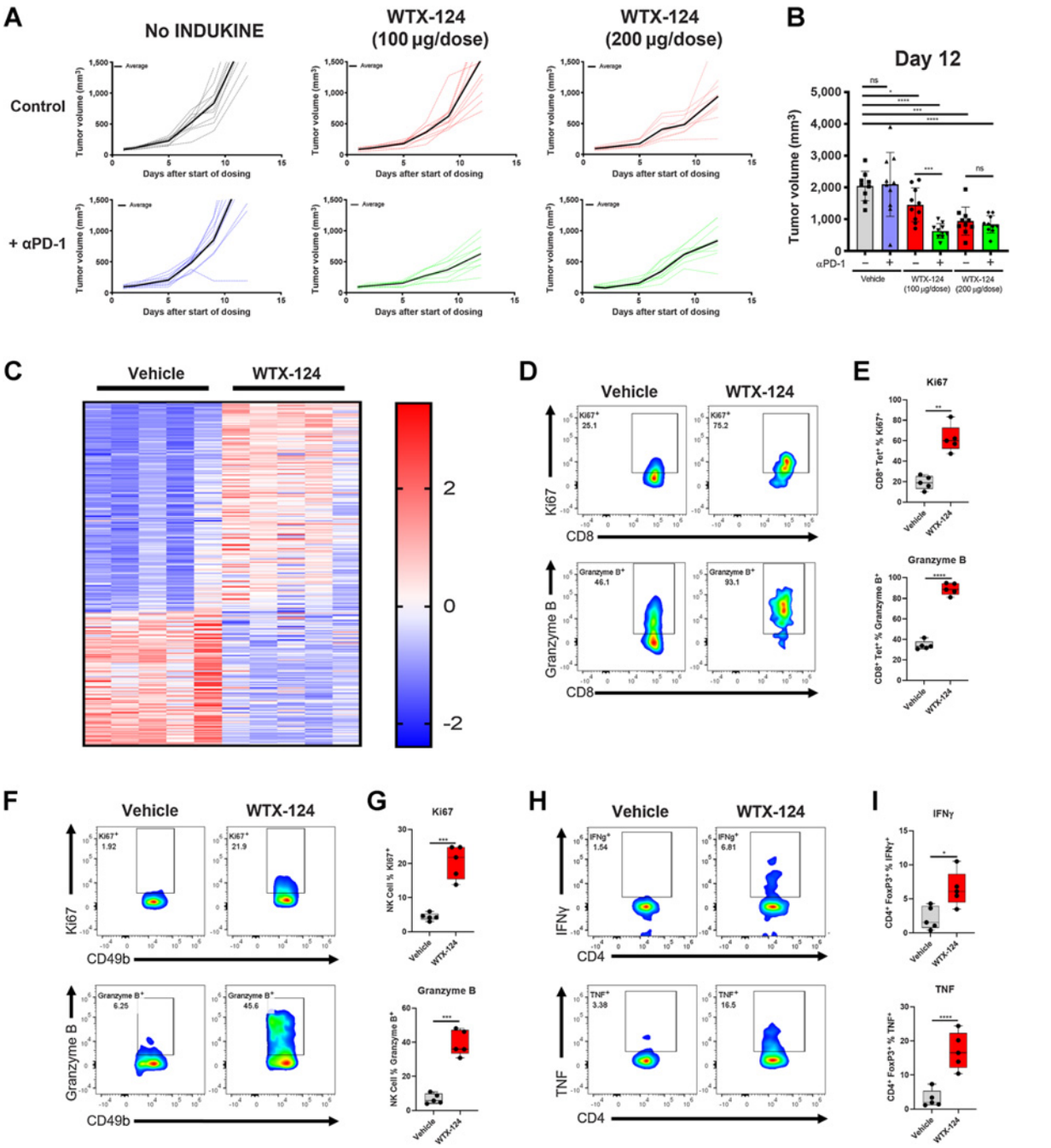

Figure 6.

WTX-124 treatment increases CD8$^+$ T-cell activation and Treg fragility in B16-F10 Tumors. B16-F10 tumors were implanted and allowed to grow to an average volume of 100–150 mm^3 before mice were randomized into treatment groups. Mice were dosed twice a week with either PBS or with various doses of WTX-124. Some mice also received PD-1 blockade in addition to WTX-124 treatment. **A,** Tumor volume was measured over time. Data from individual mice (dashed lines) are depicted with the group average presented in bold. **B,** Tumor volume on day 12. **C–I,** Tumors from mice treated with either the vehicle or WTX-124 (200 µg/dose) were harvested 24 hours after the second dose. **C,** RNA from each tumor was isolated and subjected to immune profiling with the NanoString nCounter PanCancer Mouse Immune Profiling panel. Heatmap of transcripts with statistically significant differences in expression between the two treatments. Transcripts were excluded from the heatmap if they had average normalized counts below 50. Each lane represents an individual animal. **D–I,** TILs were restimulated with PMA/Ionomycin and examined for effector cytokine production and proliferation. **D** and **E,** The frequency of tumor-infiltrating tetramer-positive CD8$^+$ T cells producing granzyme B or expressing Ki67. The tetramer used in these experiments was the same tetramer from **Fig. 4**. **F** and **G,** The frequency of tumor-infiltrating NK cells producing granzyme B or expressing Ki67. **H** and **I,** The frequency of tumor-infiltrating CD4$^+$ Tregs producing IFNγ or TNF. In plots comparing only two groups, *P* values are derived from *t* tests (*, $P < 0.05$; **, $P < 0.01$; ***, $P < 0.001$; ****, $P < 0.0001$). In plots comparing multiple groups, *P* values are derived from a one-way ANOVA followed by Dunnett multiple comparisons comparing each sample with the vehicle control (*, $P < 0.05$; ***, $P < 0.001$; ****, $P < 0.0001$).

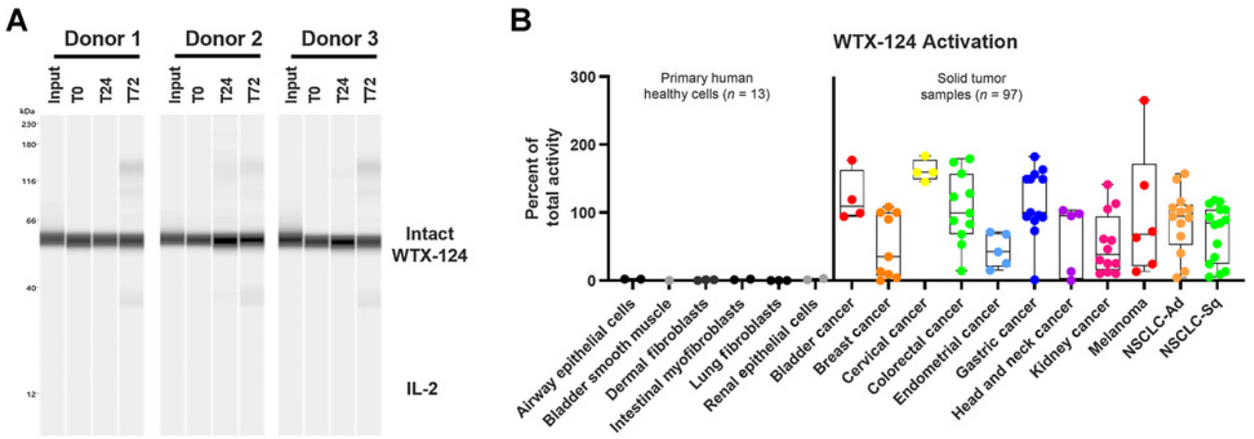

Figure 7.

WTX-124 is stable in human serum and selectively processed by primary human tumor cells. **A,** WTX-124 was diluted into healthy human serum from $n = 3$ donors and incubated at 37°C for 24 or 72 hours before WTX-124 processing was measured by Western blot analysis for IL-2. **B,** WTX-124 was exposed to primary human tumor samples ($n = 97$) or primary human healthy cells ($n = 13$) for 48 hours before INDUKINE protein cleavage was measured. Box plots represent the 25th and 75th percentile, while the line represents the median value for each indication. Whiskers represent the minimum and maximum values within a given indication. Ad, adenocarcinoma; NSCLC, non–small cell lung cancer; Sq, squamous; T, time in hours.

of cleavage, once again suggesting that this protein will be stable in the periphery in patients (**Fig. 7B**). In contrast, the majority of the tumor samples tested were able to process WTX-124. These data suggest that WTX-124 is stable when exposed to human serum or healthy primary cells but is efficiently and selectively activated by most human tumor samples, supporting its further development as an immunotherapy for patients with cancer.

Discussion

High-dose IL-2 therapy was initially approved for patients with metastatic renal cell carcinoma in 1992 and for patients with advanced melanoma in 1998 (4). Before the advent of the modern field of immuno-oncology, high-dose IL-2 stood out as a treatment associated with complete responses, albeit in a minority of patients. However, the antitumor potential of proinflammatory cytokines, like IL-2, has been hindered by the serious toxicities linked to their systemic delivery and the engagement of target cells outside the TME (4). In the case of IL-2, several pharmaceutical and biotechnology companies have tried to minimize this problem by creating less-active forms of IL-2 (known as non-α molecules) that avoid activation of the IL-2 high-affinity receptor (7–10). However, these molecular variants still systemically activate cells carrying the medium-affinity receptor (CD122/CD132 subunits), which is responsible for the signal transduction of the cytokine, and they encounter toxicity problems similar to fully active IL-2 at the doses required to see efficacy in preclinical models. As we observed with half-life extended IL-2 (WW0177), the non-α approach to IL-2 therapy may end up simply shifting the TW rather than improving it. Furthermore, newly activated $CD8^+$ T cells upregulate CD25 to form the high-affinity receptor, which is then required for their sustained expansion in the presence of antigens. This was demonstrated in a publication using a viral infection model, where $CD8^+$ T cells lacking CD25 failed to expand in infected tissues, despite expression of the medium-affinity receptor (22).

The design of WTX-124 addresses the challenges associated with rhIL-2 therapy. WTX-124 contains a native IL-2 to realize the full pharmacologic potential of this cytokine in driving antitumor immunity. The molecule is engineered as a prodrug to minimize the systemic toxicity and is conditionally activated to release IL-2 selectively in the TME. The activity of WTX-124 was highly inducible *in vitro* in a human reporter cell assay as well as in human and mouse primary cells. Likewise, WTX-124 was efficacious in mouse syngeneic models and this efficacy was dependent on tumor-specific processing. The half-life extension domain is required for the full efficacy of this molecule and provides the opportunity for better drug exposure with less frequent dosing compared with the traditional dosing schedule for high-dose IL-2 therapy (proleukin). Furthermore, despite delivering detectable levels of fully active human IL-2 into the TME, WTX-124 did not induce the VLS that was observed with equimolar amounts of either recombinant or half-life extended cytokine, demonstrating that the engineering of WTX-124 effectively blocked the systemic activity of its IL-2 component. Indeed, the peripheral inactivation provided by the IL-2 inactivation domain allowed for the safe administration of this IL-2 prodrug to mice at doses > 20-fold higher than the dose required for potent efficacy but without any obvious signs of toxicity. Between the increased efficacy and decreased toxicity, WTX-124 has a significantly wider TW than the previously described TW for high-dose IL-2.

The data reported in this publication demonstrate that WTX-124 efficacy is driven by the expansion and activation of effector cells in the tumor (both T cells and NK cells), which can produce effector cytokines such as TNF, granzyme B, and IFNγ. Indeed, activation of the tumor-infiltrating immune cells was sufficient to generate potent antitumor responses. In addition, WTX-124 treatment increased the frequency of tumor-infiltrating polyfunctional $CD8^+$ T cells, which are associated with greater cytolytic activity in viral models (18, 19). One of the concerns expressed by proponents of non-α IL-2 therapies is that CD25 is highly expressed on Tregs, and therefore Treg expansion will inhibit antitumor immunity generated in response to wild-type IL-2. Although WTX-124 treatment did result in a slight Treg expansion, the expansion of $CD8^+$ T cells far outpaced that of the Tregs, resulting in a favorable CD8/Treg ratio after treatment. Furthermore, WTX-124 treatment significantly increased the expression of IFNγ by effector cells in a tumor-specific manner. IFNγ is a fundamental effector cytokine that drives antitumor efficacy by amplifying the cellular immune component of the response and skewing $CD4^+$ T cells toward

a T_H1 phenotype. Also, more recently, it has been shown that IFNγ directs the mechanistic fragility of Tregs (20). This phenomenon was observed upon treatment with WTX-124, as the intratumoral Tregs began to produce cytokines traditionally associated with effector T cells, and it may contribute to the overall efficacy of WTX-124.

An important feature of WTX-124 is the selective processing of the prodrug in the tumor, allowing for systemic delivery, prolonged exposure, and activation of the prodrug to release fully active IL-2 in the TME. Indeed, WTX-124 was highly stable while in circulation, as shown in mice, as well as when WTX-124 was exposed to healthy primary human cells or plasma. In contrast, WTX-124 was reliably processed by primary human dissociated tumor samples from a wide variety of different cancer types, demonstrating the potential for systemically administered WTX-124 to selectively deliver IL-2 to the site of the disease and positively contribute to the development of an effective immune response.

One limitation to the data presented in this study is the reliance on two murine syngeneic tumor models, with the majority of the experiments occurring in the MC38 model. Our goal in selecting these models was not to fully examine the total range of possible responses to WTX-124 treatment, but instead to analyze models representative of "more immunogenic" and "less immunogenic" tumors. Although additional models could be explored to further examine this molecule in mice, none of the currently available murine models can accurately predict whether or not a new treatment will be effective in the clinic. Instead, these models simply provide bio-plausibility to support additional clinical development. Ultimately, the clinical benefits and safety of WTX-124 treatment will be examined in an upcoming phase I trial, subject to FDA clearance, testing WTX-124 either alone or in combination with the anti-PD-1 therapy pembrolizumab. In summary, this work presents the design features and mechanistic characteristics of WTX-124, a conditionally activated IL-2 prodrug that utilizes the dysregulated protease expression of the TME to selectively deliver full potency IL-2 to the TME following systemic administration, and to preferentially activate tumor-infiltrating immune cells to facilitate tumor rejection.

Authors' Disclosures

C.J. Nirschl reports personal fees from Werewolf Therapeutics during the conduct of the study. H.R. Brodkin reports other support from Werewolf Therapeutics during the conduct of the study; in addition, H.R. Brodkin has a patent 10,696,724 issued, a patent for PCT/US2019/032320 pending, a patent for PCT/US2019/032321 pending, and a patent for PCT/US2020/060624 pending. D.J. Hicklin reports personal fees from Werewolf Therapeutics during the conduct of the study; personal fees from MPM Capital outside the submitted work; in addition, D.J. Hicklin has a patent for PCT/US2019/032320 pending, a patent for PCT/US2020/060624 pending, a patent for PCT/US2020/032988 pending, and a patent for US10,696,724 issued. N. Ismail reports personal fees from Werewolf Therapeutics during the conduct of the study; personal fees from Werewolf Therapeutics outside the submitted work. K. Morris reports personal fees from Werewolf Therapeutics during the conduct of the study. C. Seidel-Dugan reports personal fees from Werewolf Therapeutics during the conduct of the study; in addition, C. Seidel-Dugan has a patent for US10,696,724 issued, a patent for PCT/US2019/032320 pending, a patent for PCT/US2020/060624 pending, and a patent for PCT/US2020/032988 pending. P. Steiner reports other support from Werewolf Therapeutics during the conduct of the study. Z. Steuert reports personal fees from Werewolf Therapeutics during the conduct of the study. J.M. Sullivan reports personal fees from Werewolf Therapeutics during the conduct of the study. E. Tyagi reports other support from Werewolf Therapeutics during the conduct of the study. W.M. Winston reports personal fees from Werewolf Therapeutics during the conduct of the study; personal fees from Astellas, Asylia, Stellanova, and Novasenta outside the submitted work; in addition, W.M. Winston has a patent 10,696,724 issued, a patent for PCT/US2019/032320 pending, a patent for PCT/US2020/032988 pending, and a patent for PCT/US2020/060624 pending. A. Salmeron reports other support from Werewolf Therapeutics during the conduct of the study; in addition, A. Salmeron has a patent for PCT/US2019/032320 pending and a patent for PCT/US2020/060624 pending.

Authors' Contributions

C.J. Nirschl: Conceptualization, data curation, formal analysis, supervision, investigation, visualization, methodology, writing–original draft, writing–review and editing. **H.R. Brodkin:** Data curation, formal analysis, investigation, methodology, writing–review and editing. **D.J. Hicklin:** Conceptualization, funding acquisition, writing–review and editing. **N. Ismail:** Data curation, formal analysis, investigation, methodology. **K. Morris:** Data curation, formal analysis, investigation, methodology. **C. Seidel-Dugan:** Conceptualization, writing–review and editing. **P. Steiner:** Data curation, formal analysis. **Z. Steuert:** Data curation, formal analysis, investigation, methodology. **J.M. Sullivan:** Data curation, formal analysis, investigation, methodology. **E. Tyagi:** Data curation, formal analysis, investigation, methodology. **W.M. Winston:** Conceptualization, supervision, writing–review and editing. **A. Salmeron:** Conceptualization, data curation, formal analysis, supervision, investigation, visualization, methodology, writing–original draft, project administration, writing–review and editing.

Acknowledgments

Research and analysis were supported by Werewolf Therapeutics. The authors were responsible for all content and editorial decisions and received no honoraria for development of this article. Editorial support was provided by Helen Moore of MediTech Media, funded by Werewolf Therapeutics.

The costs of publication of this article were defrayed in part by the payment of page charges. This article must therefore be hereby marked *advertisement* in accordance with 18 U.S.C. Section 1734 solely to indicate this fact.

Received October 8, 2021; revised December 22, 2021; accepted March 4, 2022; published first March 14, 2022.

References

1. Wei SC, Duffy CR, Allison JP. Fundamental mechanisms of immune checkpoint blockade therapy. Cancer Discov 2018;8:1069–86.
2. Ribas A, Wolchok JD. Cancer immunotherapy using checkpoint blockade. Science 2018;359:1350–5.
3. Pardoll DM. The blockade of immune checkpoints in cancer immunotherapy. Nat Rev Cancer 2012;12:252–64.
4. Waldmann TA. Cytokines in cancer immunotherapy. Cold Spring Harb Perspect Biol 2018;10:a028472.
5. Mitra S, Leonard WJ. Biology of IL-2 and its therapeutic modulation: mechanisms and strategies. J Leukoc Biol 2018;103:643–55.
6. Malek TR. The biology of interleukin-2. Annu Rev Immunol 2008;26:453–79.
7. Sharma M, Khong H, Fa'ak F, Bentebibel SE, Janssen LME, Chesson BC, et al. Bempegaldesleukin selectively depletes intratumoral Tregs and potentiates T cell-mediated cancer therapy. Nat Commun 2020;11:661.
8. Charych DH, Hoch U, Langowski JL, Lee SR, Addepalli MK, Kirk PB, et al. NKTR-214, an engineered cytokine with biased IL2 receptor binding, increased tumor exposure, and marked efficacy in mouse tumor models. Clin Cancer Res 2016;22:680–90.
9. Klein C, Waldhauer I, Nicolini VG, Freimoser-Grundschober A, Nayak T, Vugts DJ, et al. Cergutuzumab amunaleukin (CEA-IL2v), a CEA-targeted IL-2 variant-based immunocytokine for combination cancer immunotherapy: overcoming limitations of aldesleukin and conventional IL-2-based immunocytokines. Oncoimmunology 2017;6:e1277306.
10. Lopes JE, Fisher JL, Flick HL, Wang C, Sun L, Ernstoff MS, et al. ALKS 4230: a novel engineered IL-2 fusion protein with an improved cellular selectivity profile for cancer immunotherapy. J Immunother Cancer 2020;8:e000673.
11. Mitschke J, Burk UC, Reinheckel T. The role of proteases in epithelial-to-mesenchymal cell transitions in cancer. Cancer Metastasis Rev 2019;38:431–44.

12. Dudani JS, Warren AD, Bhatia SN. Harnessing protease activity to improve cancer care. Annu Rev Cancer Biol 2018;2:353–76.
13. Yost KE, Satpathy AT, Wells DK, Qi Y, Wang C, Kageyama R, et al. Clonal replacement of tumor-specific T cells following PD-1 blockade. Nat Med 2019; 25:1251–9.
14. Konrad MW, Hemstreet G, Hersh EM, Mansell PW, Mertelsmann R, Kolitz JE, et al. Pharmacokinetics of recombinant interleukin 2 in humans. Cancer Res 1990;50:2009–17.
15. Sands H, Loveless SE. Biodistribution and pharmacokinetics of recombinant, human 125I-interleukin-2 in mice. Int J Immunopharmacol 1989;11: 411–6.
16. Atkins MB, Lotze MT, Dutcher JP, Fisher RI, Weiss G, Margolin K, et al. High-dose recombinant interleukin 2 therapy for patients with metastatic melanoma: analysis of 270 patients treated between 1985 and 1993. J Clin Oncol 1999;17: 2105–16.
17. Ye X, Waite JC, Dhanik A, Gupta N, Zhong M, Adler C, et al. Endogenous retroviral proteins provide an immunodominant but not requisite antigen in a murine immunotherapy tumor model. Oncoimmunology 2020;9: 1758602.
18. Wherry EJ, Blattman JN, Murali-Krishna K, Van Der Most R, Ahmed R. Viral persistence alters CD8 T-cell immunodominance and tissue distribution and results in distinct stages of functional impairment. J Virol 2003;77:4911–27.
19. Imai N, Tawara I, Yamane M, Muraoka D, Shiku H, Ikeda H. CD4(+) T cells support polyfunctionality of cytotoxic CD8(+) T cells with memory potential in immunological control of tumor. Cancer Sci 2020;111: 1958–68.
20. Overacre-Delgoffe AE, Chikina M, Dadey RE, Yano H, Brunazzi EA, Shayan G, et al. Interferon-γ drives Treg fragility to promote anti-tumor immunity. Cell 2017;169:1130–41.
21. Matloubian M, Lo CG, Cinamon G, Lesneski MJ, Xu Y, Brinkmann V, et al. Lymphocyte egress from thymus and peripheral lymphoid organs is dependent on S1P receptor 1. Nature 2004;427:355–60.
22. D'Souza WN, Lefrançois L. IL-2 is not required for the initiation of CD8 T cell cycling but sustains expansion. J Immunol 2003;171:5727–35.